



INSTITUT DE FRANCE
Académie des sciences

Comptes Rendus

Chimie

Dandan Yao, Limiao Shi, Zhipeng Sun, Mireille Blanchard-Desce,
Olivier Mongin, Frédéric Paul and Christine O. Paul-Roth

**New fluorescent tetraphenylporphyrin-based dendrimers with
alkene-linked fluorenyl antennae designed for oxygen sensitization**


Volume 24, issue S3 (2021), p. 57-70

<<https://doi.org/10.5802/crchim.99>>

Part of the Special Issue: MAPYRO: the French Fellowship of the Pyrrolic
Macrocyclic Ring

Guest editors: Bernard Boitrel (Institut des Sciences Chimiques de Rennes,
CNRS-Université de Rennes 1, France) and Jean Weiss (Institut de Chimie de
Strasbourg, CNRS-Université de Strasbourg, France)

© Académie des sciences, Paris and the authors, 2021.
Some rights reserved.

 This article is licensed under the
CREATIVE COMMONS ATTRIBUTION 4.0 INTERNATIONAL LICENSE.
<http://creativecommons.org/licenses/by/4.0/>



*Les Comptes Rendus. Chimie sont membres du
Centre Mersenne pour l'édition scientifique ouverte*
www.centre-mersenne.org



MAPYRO: the French Fellowship of the Pyrrolic Macrocyclic Ring / *MAPYRO: la communauté française des macrocycles pyrroliques*

New fluorescent tetraphenylporphyrin-based dendrimers with alkene-linked fluorenyl antennae designed for oxygen sensitization

Dandan Yao^a, Limiao Shi^a, Zhipeng Sun^a, Mireille Blanchard-Desce^{*, b},
Olivier Mongin^{*, a}, Frédéric Paul^{*, a} and Christine O. Paul-Roth^{*, a}

^a Univ Rennes, INSA Rennes, CNRS, ISCR (Institut des Sciences Chimiques de Rennes) – UMR 6226, F-35000 Rennes, France

^b Université de Bordeaux, Institut des Sciences Moléculaires (CNRS UMR 5255), 33405 Talence, France

E-mails: ydd000@126.com (D. Yao), lmshi09@yahoo.com (L. Shi), sunzpciomp@126.com (Z. Sun), mireille.blanchard-desce@u-bordeaux.fr (M. Blanchard-Desce), olivier.mongin@univ-rennes1.fr (O. Mongin), frederic.paul@univ-rennes1.fr (F. Paul), christine.paul@univ-rennes1.fr, christine.paul@insa-rennes.fr (C. O. Paul-Roth)

Abstract. The design of porphyrin-based dendrimers featuring conjugated fluorenyl dendrons *via* alkene spacers allows evaluating the importance of the role of these spacers on the optical properties of interest. In the continuation of previous studies, a second-generation porphyrin-based dendrimer was synthesized and metalated by Zn(II) along with its known first-generation homologue. The targeted free-base porphyrin was obtained by repetitively cycling a Michaelis–Arbuzov reaction and a Horner–Wadsworth–Emmons reaction to construct the desired vinyl-containing dendrons. After metalation by Zn(II), *meso*-tetraphenylporphyrin-cored dendrimers with eight (**ZnTPP-D1**) and sixteen (**ZnTPP-D2**) fluorenyl arms at their periphery were eventually isolated. These species allow evaluating the influence of the central metal and of the 1,2-alkyne for 1,2-alkene exchange on fluorescence, oxygen photosensitization, and two-photon absorption. Such structure–property relationships are currently needed for the design of optimal dendrimeric photosensitizers allowing combined two-photon-based photodynamic therapy (2P-PDT) and imaging.

Keywords. Porphyrin, Fluorenyl, Fluorescence, Energy transfer, Double bond, Dendrimer, Photodynamic therapy.

Available online 30th July 2021

1. Introduction

There has been great interest in porphyrin systems because the peripheral substituents on the

macrocyclic core allows to significantly modulate the photophysical properties at will. Thus, light-harvesting compounds can be easily obtained by attaching four strongly absorbing energy-donor dendrons at the *meso* positions of the central porphyrin core which will play the role of peripheral

* Corresponding author.

“antenna” [1–3]. In this respect, Fréchet and coworkers [4–6] have reported porphyrin systems with fluorene-containing oligoether-type dendrons as efficient one- and two-photon light-harvesting units and demonstrated that such an “antenna effect” was facilitated in dendritic architectures *versus* linear architectures [5,6]. More recently, related star-shaped porphyrins with fully conjugated oligofluorene arms have also been reported by Bo and coworkers and shown to behave as a remarkable light-harvesting system [7–9].

In this context, we have previously reported the synthesis of porphyrin possessing four fluorenyl arms directly connected at the *meso*-positions. This compound (**TFP**; Figure 1a) [10,11] exhibited a high luminescence quantum yield (24%), demonstrating the good capacity of the fluorenyl units to enhance emission by increasing the radiative process [12]. Subsequently, we synthesized two series of substituted *meso*-porphyrin dendrimers with terminal fluorenyl arms, taking **TPP** as the central unit: (i) a non-conjugated family with flexible ether linkages [13–15] and, more recently, (ii) a conjugated family with rigid alkynyl linkages (Figure 1b) [16,17]. We could then show that these molecular architectures were promising models for the design of new biphotonic photosensitizers for theranostics, *i.e.*, allowing to perform photodynamic therapy [18,19] and fluorescence imaging after two-photon excitation [16,17]. Due to the practical advantages of two-photon excitation, this field has attracted attention and is rapidly expanding; several such porphyrin-based photosensitizers have been reported to date [20–26]. In order to gain additional insight about the potential of TPP-cored dendrimers such as **TPP-T1** or **TPP-T2** in this field, we have started systematically investigating the impact of various structural changes taking place in the peripheral light-harvesting antenna on the photophysical properties of these systems.

Given that 1,2-alkene spacers are known to promote electronic communication better than 1,2-alkyne ones [27], we recently started exploring the optical properties of related dendrimers featuring alkene linkages. However, this was exclusively done for the *first-generation* dendrimer **TPP-D1** (Figure 1c; $M = 2H$) resulting in a significant improvement in the linear and nonlinear optical properties *versus* **TPP-T1** [28]. This statement prompted us to test higher generation dendrimers of this kind.

Accordingly, we now report our efforts to isolate the *second-generation* dendrimer **TPP-D2** and the corresponding metalated species **ZnTPP-D1** and **ZnTPP-D2**. Subsequently, their linear and nonlinear optical properties of interest will be disclosed as well as evidence for the very efficient energy-transfer process taking place from the conjugated dendrons to the porphyrin core in these new species. These data will then be compared to those of their known alkyne-containing analogs (or **T** series; Figure 1b).

2. Results and discussion

2.1. Synthesis and characterization

This new family of dendrimers was prepared by the synthesis of the required dendrons (**D1-PhCHO** and **D2-PhCHO**), followed by their condensation with pyrrole to give the desired free-base porphyrins as intermediates, which were then metalated by Zn(II) to give the final dendrimers **ZnTPP-D1** and **ZnTPP-D2**.

2.1.1. Dendron synthesis

The synthesis of the two generations of vinyl-bridged aldehyde-terminated dendrons **D1-PhCHO** and **D2-PhCH** is described in Scheme 1. First, commercial 1-bromo-3,5-bis(methyl)benzene was halogenated with benzyl by *N*-bromosuccinimide (NBS) using azobis-isobutyronitrile (AIBN) as the radical initiator. Given that this bromination takes place usually non-selectively [29–32], the reaction conditions were optimized (temperature, time, and solvent). The resulting conditions mainly gave the desired dibrominated product along with mono- and tribrominated byproducts. The former byproduct could be isolated by chromatography (heptane), while the latter could not be fully separated from the targeted dibrominated product (ratio tri/di of 1/4 by 1H NMR). In the next step, this mixture containing 49% of the desired product was reacted directly with excess of $P(OEt)_3$ under reflux following a Michaelis–Arbuzov [29–31] protocol. The desired product **3** and its bromo-substituted byproduct were both formed and were subsequently separated by chromatography (Scheme 1). The unwanted byproduct could be easily eluted using CH_2Cl_2 , while the target product **3** was collected using ethyl acetate as a colorless oil in 83% yield. After a subsequent Horner–Wadsworth–Emmons (HWE) reaction [29–31], the compound **3**

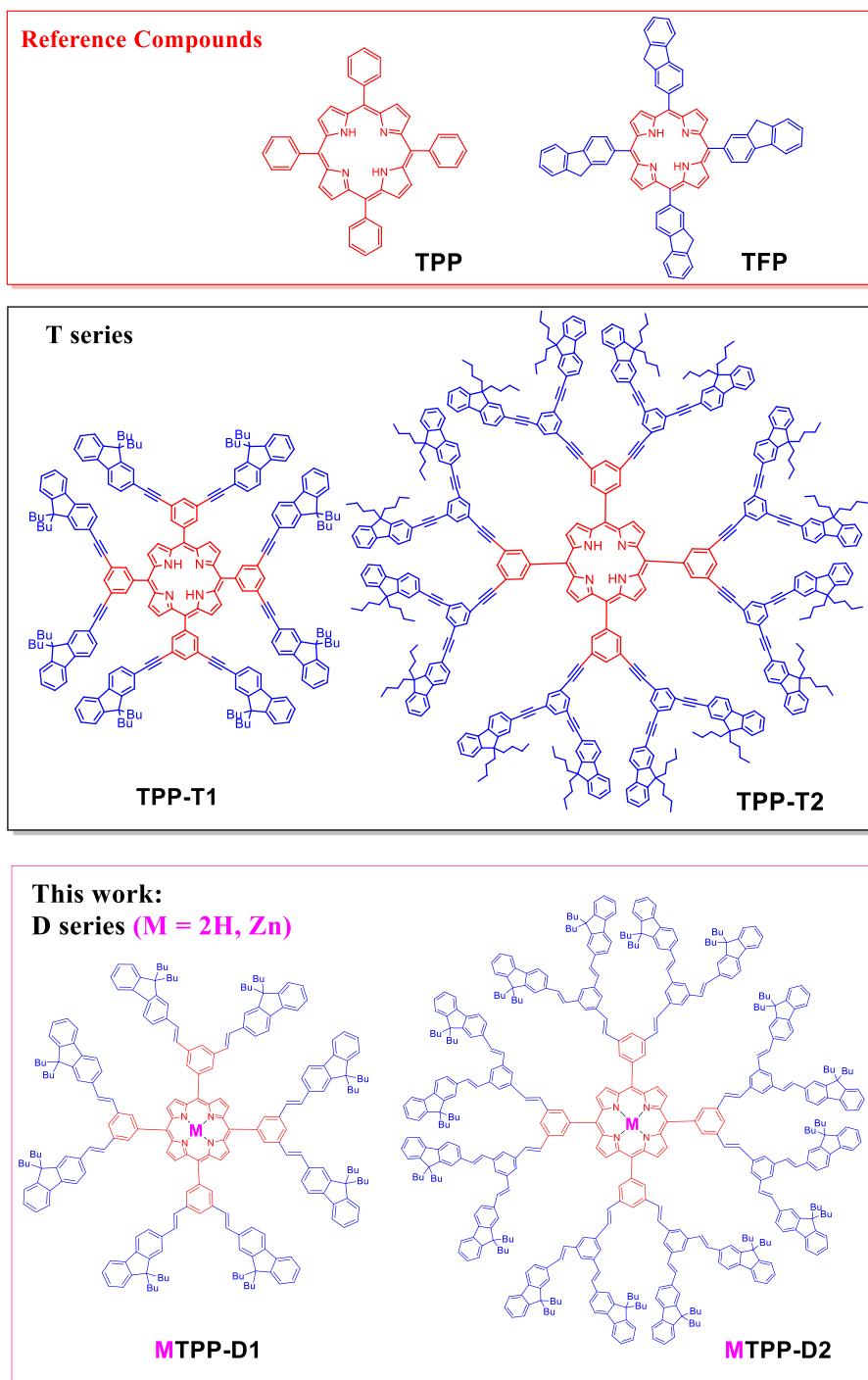
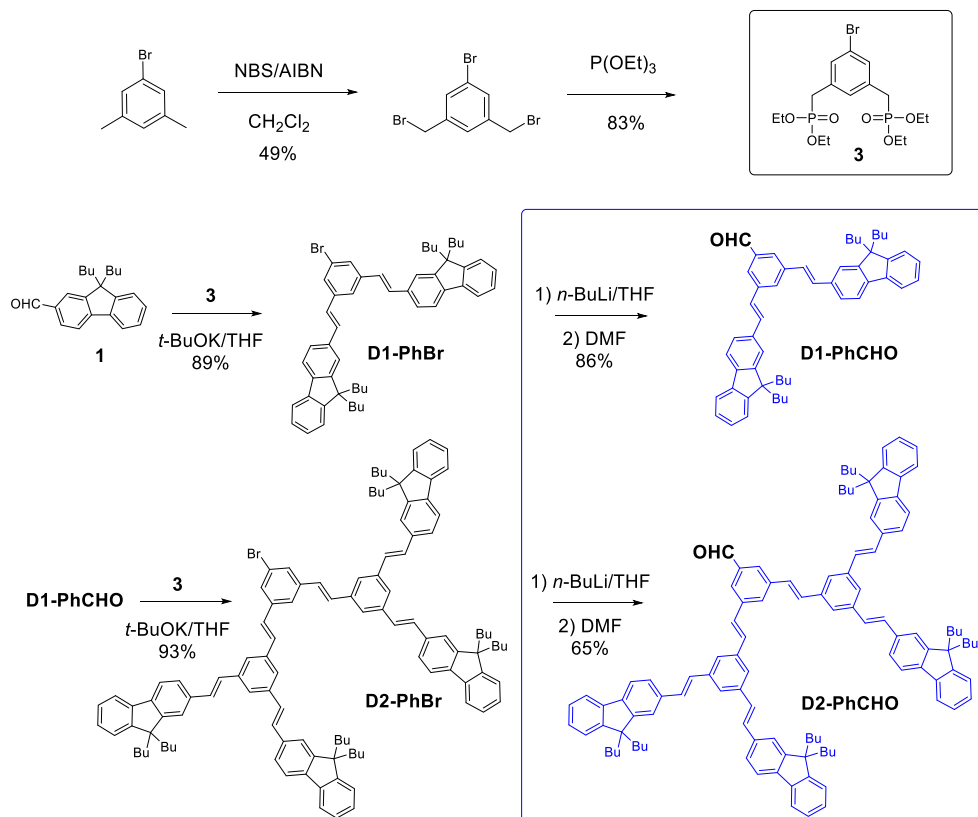


Figure 1. (a) Reference compounds; (b) previously reported alkyne-bridged free-base porphyrin dendrimers (**T series**) based on TPP (**TPP-T1** and **TPP-T2**); (c) new porphyrin dendrimers (**D series**) based on TPP (**MTPP-D1** and **MTPP-D2**; M = 2H, Zn).



Scheme 1. Synthetic routes for alkene-bridged dendrons **D1-PhCHO** [28] and **D2-PhCHO**.

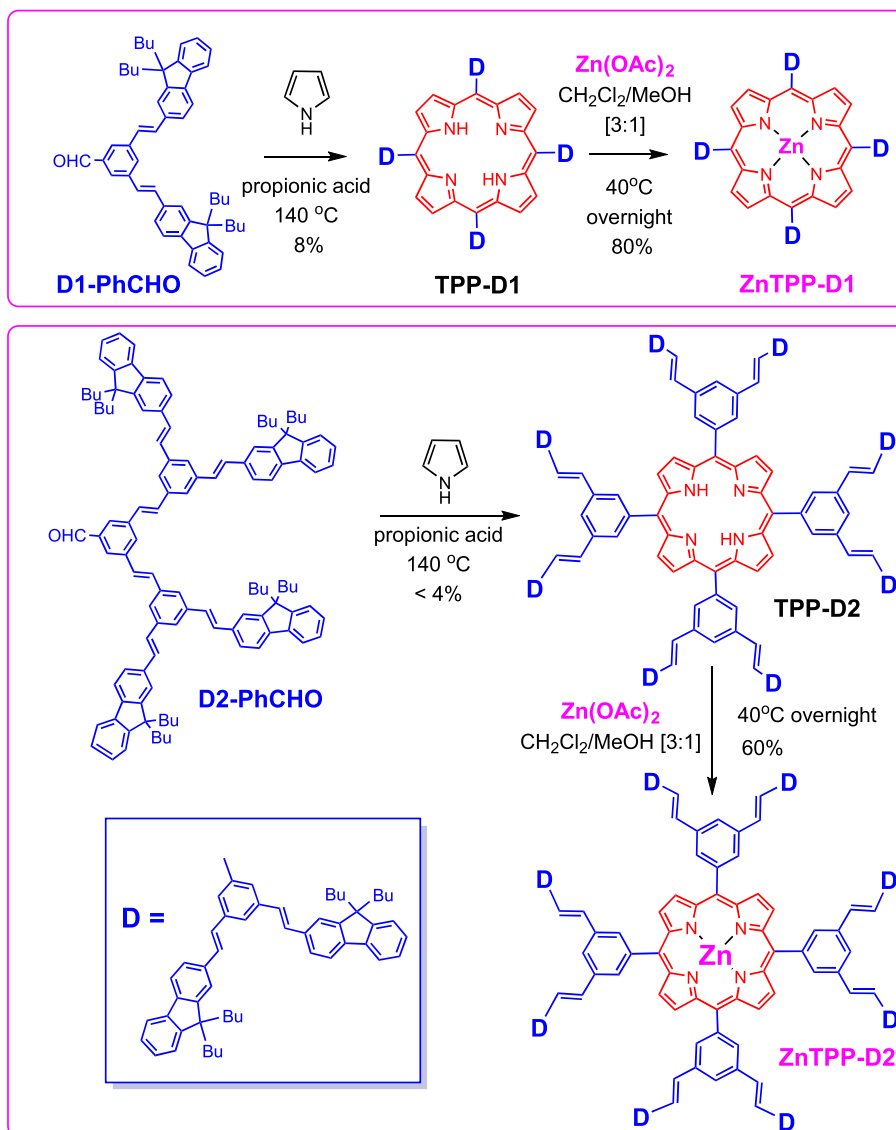
reacts with the previously prepared aldehyde **1** [16] in the presence of *t*-BuOK/THF to give the double-bonded precursor **D1-PhBr** in 89% yield. The aldehyde **D1-PhCHO** can then be obtained in two steps from this product in 86% yield. Repetition of the HWE reaction [29–31] between this new aldehyde and **3** gave access to the *second-generation* intermediate **D2-PhBr** in 93% yield, and subsequently to the corresponding **D2-PhCHO** dendron in 65% yield (Scheme 1).

2.1.2. Porphyrin synthesis

Two synthetic methods are most often used to synthesize porphyrins: the Adler–Longo [33,34] or the Lindsey reaction [35]. Both are efficient for synthesizing porphyrins substituted at their *meso* positions. Given that the *first-generation* dendrimer **TPP-D1** was previously isolated using the Adler–Longo approach [28], these reaction conditions were used again to synthesize **TPP-D2**. However, this compound could not be isolated in pure form even

after several purification attempts by chromatography and subsequent recrystallizations (CHCl₃ and MeOH), the yield of crude **TPP-D2** in the isolated solid being below 4%. Fortunately, all these porphyrin dendrimers have good solubilities in common organic solvents, allowing their easy metalation, and this approach provided a way to access the pure zinc complex from the mixture in the case of **ZnTPP-D2** (Scheme 2). Thus, the corresponding zinc complex **ZnTPP-D1** was formed at 40 °C overnight from **TPP-D2** using Zn(OAc)₂ in CH₂Cl₂/MeOH and isolated pure in 60% yield (Scheme 2). Using similar conditions for metalation, **ZnTPP-D1** was isolated in 80% yield from **TPP-D1**.

From a purely synthetic standpoint, the isolated yields in alkene-bridged dendrimers (**D**-type series; Figure 1c) were always lower than those of their alkyne-bridged analogs (**T**-type series; Figure 1b), although rigorously similar reaction conditions have been used (the isolated yields of **TPP-T1** and **TPP-T2** were 18% and 13%, respectively [16,17]), making the



Scheme 2. Synthesis of vinyl-bridged porphyrin dendrimers (**D** series) based on TPP-cored porphyrin (**TPP-D1** and **TPP-D2**) and corresponding zinc(II) complexes (**ZnTPP-D1** and **ZnTPP-D2**).

D-type series dendrimers more challenging to obtain *via* the Adler–Longo approach [16,17,36].

2.1.3. ¹H NMR analysis

The aldehyde dendrons **D1-PhCHO** and **D2-PhCHO**, and the corresponding dendrimers, *i.e.*, the free-base and metalated porphyrins **MTPP-D1** and **MTPP-D2**, were characterized by ¹H NMR analysis (Figures 2–4). Figure 2 shows the full ¹H NMR spectra of the dendrons compared to those of their analogs

with triple bonds (**T1-PhCHO** and **T2-PhCHO**). They all show three diagnostic signatures: (i) the aldehyde proton as a singlet, around 10 ppm; (ii) the aromatic protons located as multiplets, in region 7–8 ppm, belonging to protons of phenyl and fluorenyl, partially identified; (iii) four groups of alkyl protons H_{a,b,c,d} located at 0.5–2.1 ppm that are assigned to the *n*-butyl chains of fluorenyl. We can particularly notice that for the double-bonded dendrons **D1-PhCHO** and **D2-PhCHO**, we observe four additional

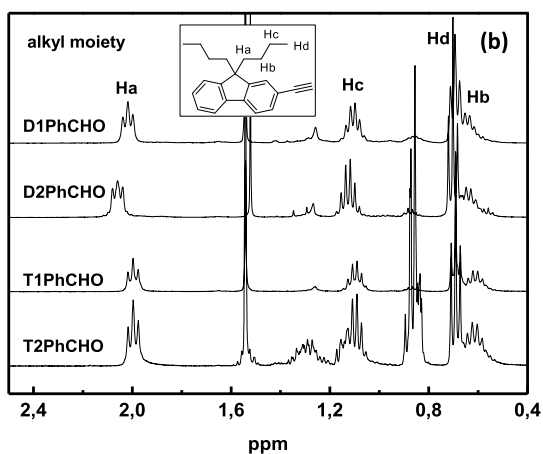
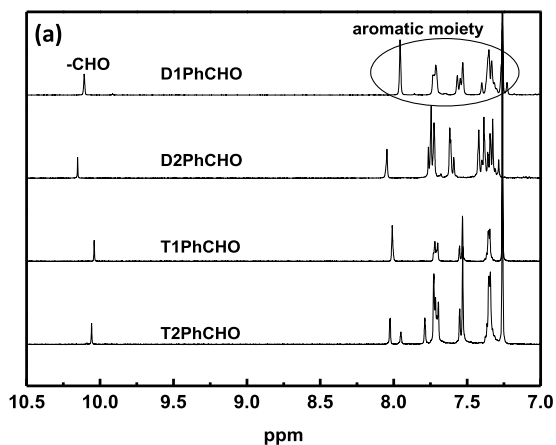


Figure 2. Aromatic (a) and Alkyl (b) moieties ^1H NMR spectra (400 MHz) of **D**-series dendrons **D1-PhCHO** and **D2-PhCHO** compared to reported **T**-series dendrons **T1-PhCHO** and **T2-PhCHO** in CDCl_3 [16,17].

alkene protons coming out as a broad peak around 7.18–7.40 ppm.

The full ^1H NMR spectra in CDCl_3 of the corresponding free-base porphyrin **TPP-D1** (Figure 3) shows four diagnostic signatures: (i) the β -pyrrolic protons of the porphyrin core (H_β) around 9 ppm, (ii) the aromatic protons around 7.3–8.4 ppm, (iii) the alkyl protons of the various butyl chains around 2.2–0.5 ppm, and (iv) the NH protons of porphyrin cavity around -2.6 ppm. For **TPP-D1**, as for reported **TPP-T1** and **TPP-T2** [16,17], we observe eight protons H_β of porphyrin ring located around 9 ppm. For aromatic and vinylic protons (around 7.2–8.4 ppm),

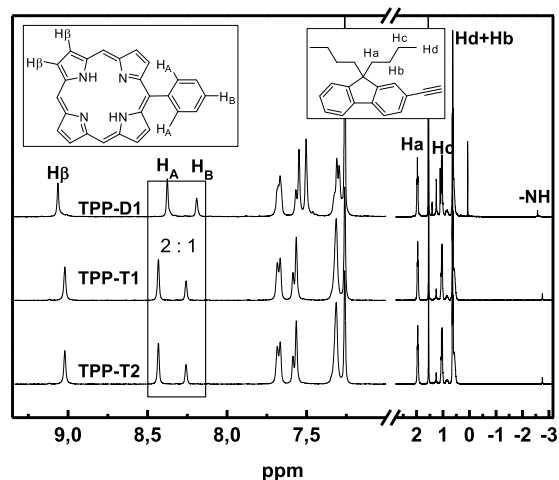


Figure 3. Full ^1H NMR spectra (400 MHz) of the free-base TPP-cored dendrimers **TPP-D1**, **TPP-T1**, and **TPP-T2** in CDCl_3 .

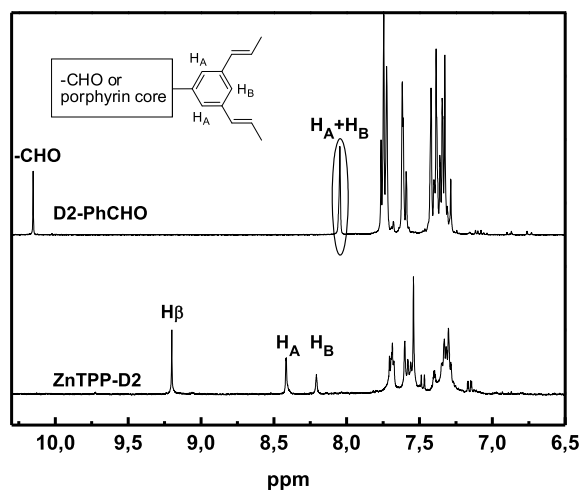


Figure 4. Partial ^1H NMR spectra (400 MHz) of the dendron **D2-PhCHO** and of the corresponding zinc(II) complex **ZnTPP-D2** in CDCl_3 .

only some of them can be easily assigned like H_A and H_B . Again, the vinyl protons of **TPP-D1** give rise to a broad peak around 7.2–7.3 ppm. For all these dendrimers, the *n*-butyl protons ($\text{H}_{\text{a,b,c,d}}$) are simply assigned to four groups of signals located at 0.5–2.1 ppm as for the corresponding dendrons. In contrast, for the larger dendrimer **TPP-D2**, a ^1H NMR spectrum with broad signals was obtained (see ESI)

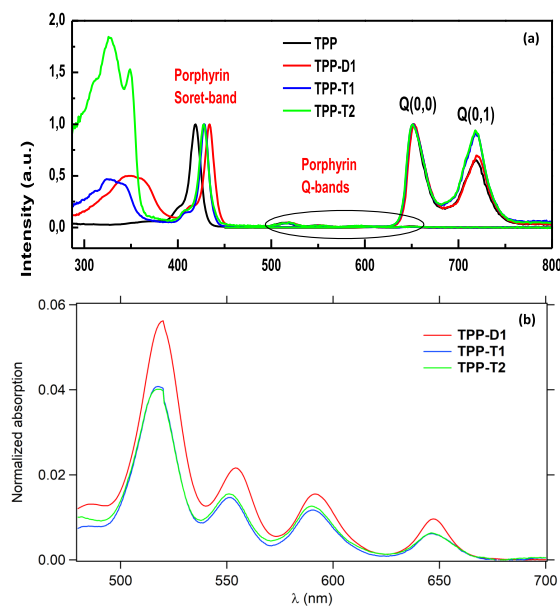


Figure 5. Normalized absorption and emission spectra of selected TPP-cored dendrimers (**TPP-D1**, **TPP-T1**, and **TPP-T2**) compared to reference **TPP** in toluene (a). Detail of the Q-bands of **TPP-D1**, **TPP-T1**, and **TPP-T2** (b).

and only for the corresponding zinc(II) complex **ZnTPP-D2** the spectrum was well resolved (Figure 4). Some characteristic signals are also readily identified; (i) eight protons H_{β} of porphyrin ring located around 9 ppm, (ii) H_A and H_B in the phenyl arms. However, most of the aromatic and vinylic protons overlap (7.2–8.4 ppm) because of the larger molecular structure.

2.2. Photophysical properties

UV-visible absorption and emission spectra, after excitation in the Soret band [37,38], were recorded for the isolated dendrimers at room temperature (Table 1 and Figures 5 and 6). The free-base tetraphenylporphyrin (**TPP**; Figure 1a) and the corresponding zinc complex (**ZnTPP**) were chosen as references compounds. Their two-photon oxygen-photosensitizing yields were subsequently evaluated and compared to those of their alkyne analogs (**TPP-T1** and **TPP-T2**) to analyze the impact of this structural modification (Tables 2–3).

For the free-base porphyrin series, all absorption spectra are typical of porphyrin derivatives with an

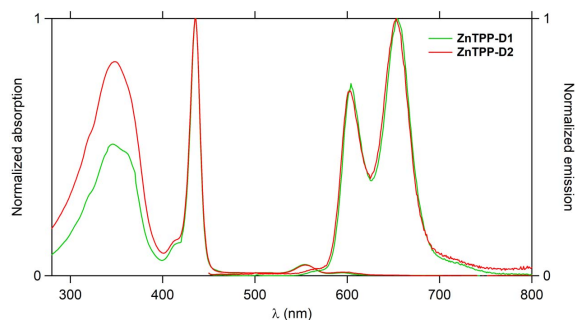


Figure 6. Absorption and emission spectra of **ZnTPP-D2** compared to **ZnTPP-D1** in CH_2Cl_2 at 20 °C.

intense Soret band around 430 nm and four Q-bands in the 520–650 nm range [37]. Compared to **TPP**, the dendrimers **TPP-D1**, **TPP-T1**, and **TPP-T2** present an additional absorption around 300–400 nm, corresponding to the conjugated fluorenyl dendrons. This band is almost of similar intensity for **TPP-D1** and **TPP-T1**, most likely in reason of their identical terminal fluorenyl number; however, a red shift is observed for **TPP-D1** compared to **TPP-T1**, likely due to the improved conjugation between core and arms in the former compound. Concerning the Soret band, the vinyl-bridged dendrimer **TPP-D1** presents also a larger red shift (15 nm) than its alkyne analog **TPP-T1** (9 nm) *versus* the Soret band of the reference **TPP**, which reflect the extension of the porphyrin π manifold [40] through conjugation with the peripheral arms at the *meso* positions.

The corresponding zinc complexes **ZnTPP-D1** and **ZnTPP-D2** exhibit characteristic changes in their electronic spectra compared to those of the corresponding free-base porphyrins **TPP-D1** and **TPP-D2** [37,41]. Only two Q-band absorption are now observed, around 552 nm and 635 nm, due to the symmetry change from D_{2h} to D_{4h} symmetry upon metalation and an intense Soret band around 435 nm (Table 1 and Figure 6). An additional broad band is also observed in UV range (346 nm) which corresponds to π – π^* absorption of the fluorenyl chromophores. This UV absorption is weaker for the *first-generation* zinc(II) complex (**ZnTPP-D1**) than for the higher generation dendrimer (**ZnTPP-D2**) due to the smaller number (eight *versus* sixteen) of fluorenyl groups present in the peripheral arms.

Upon excitation in their Soret band, all these compounds exhibit the characteristic porphyrin

Table 1. Photophysical properties of the new dendrimers **TPP-D1**, **ZnTPP-D1**, **ZnTPP-D2** compared to their alkynyl-bridged parents **TPP-T1** and **TPP-T2** and to **TPP** reference at 20 °C [16,17,36]

	Absorption ^a (nm)			Emission ^a		Quantum yield ^b Φ_F (%)
	Dendron	Soret band	Q-bands	Ex = Soret band Q(0,0)	Q(0,1)	
TPP	—	419	514, 548, 590, 649	652	719	11
ZnTPP	—	421	556, 603	603	650	3
TPP-D1	349	434	518, 552, 593, 649	652	719	13
ZnTPP-D1^c	346	436	554, 594	604	654	3
ZnTPP-D2^c	348	435	555, 595	602	652	6
TPP-T1	325	428	518, 552, 593, 649	652	719	12
TPP-T2	327, 349	428	518, 552, 593, 649	652	719	13

^aUnless precised, experiments were achieved in toluene (HPLC level) with the UV-visible absorption region from 287 to 800 nm and emission region from 450 to 800 nm.

^bUnless precised, experiments for fluorescence quantum yields were achieved in toluene (HPLC level) using TPP ($\Phi = 11\%$) as standard, by Soret-band excitation [12].

^cData obtained in CH₂Cl₂ (HPLC level).

Table 2. Two-photon absorption and brightness properties of **D** dendrimers and related **T** compounds in dichloromethane

Compound	Fluorenes/ porphyrin	$\lambda_{\text{TPA}}^{\text{max}}$ (nm)	σ_2^{max} (GM) ^a	$\Phi_F \cdot \sigma_2^{\text{max}}$ (GM) ^b	Two-photon brightness enhancement factor ^c
TPP	0	790	12 ^d	1.3	1
TPP-D1	8	790	280	36	28
ZnTPP-D1	8	790	260	8	6
ZnTPP-D2	16	810	450	27	20
TPP-T1	8	790	200	24	18
TPP-T2	16	790	290	38	29

^aIntrinsic TPA cross-sections measured in 10⁻⁴ M dichloromethane solutions by TPEF in the femtosecond regime; a fully quadratic dependence of the fluorescence intensity on the excitation power is observed and TPA responses are fully non-resonant.

^bMaximum two-photon brightness in dichloromethane.

^cEnhancement factor: $\Phi_F \sigma_2^{\text{max}}$ of the compound normalized to that of **TPP**.

^dData from lit [39].

emission peaks Q(0,0) and Q(0,1) [12,40]. After normalizing their emission spectra on their Q(0,0) peaks, these compounds exhibit two emission peaks at similar wavelengths, but with different intensities (Figure 5). Compared to **TPP**, the Q(0,1) band of all dendrimers does not change in intensity for **TPP-D1** but increases for **TPP-T1** and **TPP-T2**. The emission spectra of zinc(II) porphyrin complexes usually

consist of three sub-bands assigned to a vibronic progression from a Q state: Q(0,0), Q(0,1), and weak Q(0,2), the last one, near 720 nm being usually too weak to be observed [11]. Presently, for **ZnTPP-D1** and **ZnTPP-D2**, the emission spectra exhibit the two expected Q-bands around 603 nm and 653 nm (Figure 6), the blue shift of these bands compared to the corresponding free bases being ascribable to the

Table 3. Oxygen sensitization properties of double-bonded porphyrin dendrimers and related triple-bonded compounds

Compound	Φ_{Δ}^a (%)	$\Phi_{\Delta} \cdot \sigma_2^{\max}$ (GM) ^b	Two-photon excited oxygen sensitization enhancement factor ^c
TPP	60	7.2	1
TPP-D1	64	177	25
ZnTPP-D1	59	153	21
ZnTPP-D2	55	248	34
TPP-T1	59	118	16
TPP-T2	56	162	23

^aSinglet oxygen production quantum yield determined relative to **TPP** in dichloromethane (Φ_{Δ} [TPP] = 0.60).

^b $\Phi_{\Delta} \sigma_2^{\max}$: figure of merit of the two-photon excited singlet oxygen production in dichloromethane.

^cEnhancement factor: $\Phi_{\Delta} \sigma_2^{\max}$ of the compound normalized to that of **TPP**.

metal coordination. The quantum yields (Φ_F) were then measured for all these compounds (Table 1). While the free-base porphyrin dendrimers have similar quantum yields ($\Phi_F = 12$ –13%) than **TPP** ($\Phi_F = 11\%$), these values drop drastically (3–6%) when a metal like zinc(II) is introduced in the porphyrin cavity, as also observed for the reference **ZnTPP**.

The existence of an energy-transfer (ET) process from the peripheral 2-fluorenyl donors toward the central porphyrin acceptor core was subsequently studied. The emission spectra were measured from 450 to 800 nm, using two excitation wavelengths: the dendron absorption (325–351 nm) and the Soret-band absorption (419–434 nm). As expected, all dendrimers showed exclusive Q-band emission around 650–720 nm, in both cases, with no residual dendron emission (usually observed around 400 nm). This suggests that the peripheral fluorenyl groups transfer their energy very efficiently to the porphyrin core, given that any dendron emission is totally quenched (SI Figure S14). This very efficient energy transfer most likely corresponds to a so-called “through-bond” energy-transfer process (TBET) [42]. Thanks to this very efficient “antenna effect”, the dendron absorption band, when intense (as in **ZnTPP-D2**), might be efficiently used for exciting these compounds.

2.3. Two-photon absorption

As these dendrimers exhibit good fluorescence properties, their intrinsic two-photon absorption cross-

sections were determined by two-photon excited fluorescence (TPEF) in CH_2Cl_2 . Measurements were performed with 10^{-4} M solutions, using a mode-locked Ti:sapphire laser delivering femtosecond pulses, following the experimental protocol described by Xu and Webb [43]. A fully quadratic dependence of the fluorescence intensity on the excitation power was observed for each sample at all the wavelengths of the spectra (790–920 nm), indicating that the cross-sections determined are only due to TPA. A significant increase of their TPA cross-sections compared to that of **TPP** (12 GM at 790 nm) was observed for all porphyrins possessing fluorenyl dendrons (Table 2 and Figure 7). Comparison between the free-base dendrimers **TPP-D1** and **TPP-T1** reveals that replacing triple bonds with double bonds in the peripheral dendrons leads to a significant increase of the TPA cross-sections.

The zinc complexes of the **D**-type series (**ZnTPP-D1** and **ZnTPP-D2**) also exhibit high TPA cross-sections ($\sigma_2 = 260$ and 450 GM, respectively) at 790 nm, **ZnTPP-D2** being the best two-photon absorber of the series of compounds presently investigated. From the comparison between **TPP-D1** and **ZnTPP-D1**, metalation by Zn(II) does not result in a significant change in cross-section at this wavelength and induces a slight decrease of σ_2 at higher wavelengths compared to the corresponding free-base porphyrin. This statement suggests that the cross-section of the missing **TPP-D2** free-base porphyrin would be similar or slightly above that of **ZnTPP-D2**

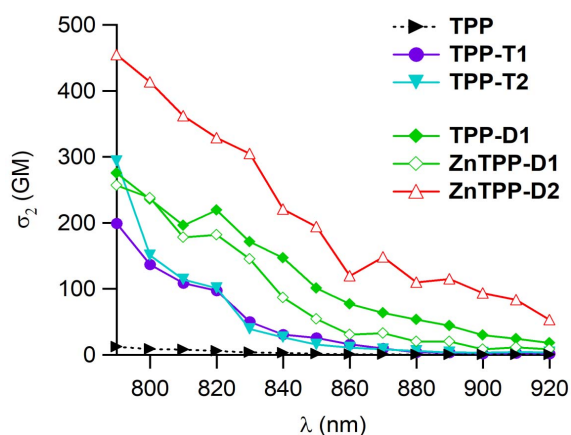


Figure 7. Two-photon excitation spectra of **D** dendrimers **TPP-D1**, **ZnTPP-D1**, and **ZnTPP-D2** and comparison with related **T** compounds **TPP-T1**, **TPP-T2**, and reference **TPP** in dichloromethane.

in the 790–920 nm range. In this respect, the clear enhancement of σ_2 observed for **ZnTPP-D2** relative to **ZnTPP-D1** is particularly remarkable. First, it reveals a more pronounced structural difference in two-photon cross-sections for the **D**-type series than for the **T**-type series, in favor of the largest dendrimers. Then it suggests that the free-base dendrimer **TPP-D2** would be a better two-photon absorber than its **TPP-T2** analog in the investigated wavelength range.

The two-photon brightness ($\sigma_2 \cdot \Phi_F$) is a figure of merit allowing the evaluation of the potential of two-photon absorbers for fluorescence imaging. For the zinc complexes, any change in σ_2 is combined with a strong decrease in Φ_F leading to a decrease of this figure of merit for **ZnTPP-D1** relative to that of its free-base analog **TPP-D1**, which is the highest of the compound presently discussed. The **ZnTPP-D2** dendrimer still exhibits an interesting two-photon brightness which is enhanced more than 20 times compared to **TPP** used as reference. Among free-base porphyrins, the two-photon brightness of **TPP-D1** is also significantly higher than that of its analog **TPP-T1**, revealing the positive impact of replacing triple bond by double bonds in the peripheral dendrons for imaging purposes.

The oxygen-photosensitizing properties of these dendrimers were also studied. Their quantum yields of singlet oxygen generation (Φ_Δ) were determined

and compared to those of analogous **T** dendrimers and **TPP** used as reference (Table 3). All these dendrimers exhibit values comprised between 0.55 and 0.64, comparable to that of reference **TPP** (0.60). Interestingly, the free-base dendrimer **TPP-D1** shows the highest value $\Phi_\Delta = 64\%$, whereas the two zinc complexes **ZnTPP-D1** and **ZnTPP-D2** show the lowest ones (59% and 55%, respectively). As previously noticed for **T**-type dendrimers [16,17,36], the increase in fluorescence quantum yield of the new free-base dendrimer **TPP-D1** relative to **TPP** is not obtained at the expense of the singlet oxygen production.

In combination with the notable increase of the TPA cross-sections of the dendrimer **TPP-D1** compared to its **TPP-T1** analog, significant enhancements of the figure of merit for the two-photon excited oxygen sensitization ($\Phi_\Delta \cdot \sigma_2^{\text{max}} = 177 \text{ GM}$) can be achieved. For the zinc complexes, this value goes up to 153 GM for **ZnTPP-D1** and even to 248 GM for larger **ZnTPP-D2**. The free-base **TPP-D1** dendrimer exhibits a clearly higher enhancement factor than its **T**-type analog, in relation with its higher σ_2 and its slightly increased Φ_Δ . This compound, easy to synthesize, appears therefore particularly promising for two-photon photodynamic therapy, and, considering its TPEF properties, also for theranostic applications provided it can be made water-soluble by proper functionalization. It should be emphasized that other porphyrin-based systems with more efficient conjugation between the sub-chromophoric units have often been shown to exhibit higher TPA cross-sections, but these are generally accompanied by strong modifications of their other photophysical properties such as the red shift of their linear absorption range [24,44–51], which somewhat limits their interest for theranostics. Indeed, most often these highly efficient two-photon absorbers exhibit a modest to negligible fluorescence or some interfering residual one-photon absorption above 800 nm, which leads to the loss of the 3D resolution. In contrast, the dendrimers presently reported, with a more restricted π -conjugation between the dendrons and the porphyrin core,¹ exhibit an improved

¹There is a large dihedral angle between the *meso*-aryl substituent and the macrocycle, which is more than 60° in the case of **TPP**, see [52].

trade-off [16,17,36,53] between intrinsic TPA, fluorescence, and photosensitizing properties.

3. Experimental section

3.1. General

Unless otherwise stated, all solvents used in reactions were distilled using common purification protocols [54], except DMF and $^i\text{Pr}_2\text{NH}$, which were dried on molecular sieves (3 Å). All chromatographic separations were effected on silica gel (40–60 μ , 60 Å). ^1H and ^{13}C NMR spectra were recorded on BRUKER Ascend 400 and 500 at 298 K. The chemical shifts are referenced to internal tetramethylsilane. High-resolution mass spectra were recorded on Bruker MicrOTOF-Q II in ESI positive mode in dried solvent at CRMPO in Rennes. Reagents were purchased from commercial suppliers and used as received. Element analyses were collected on a Microanalyser Flash EA1112. UV-visible absorption and photoluminescence spectroscopy measurements for all porphyrin dendrimers in solution were performed on Edinburg FLS920 Fluorimeter (Xe900) and BIO-TEK instrument UVIKON XL spectrometer at room temperature. Toluene and dichloromethane for spectral analysis were HPLC grade.

3.2. Dendron synthesis and characterization

The two dendrons **D1-PhCHO** and **D2-PhCHO** were obtained after a multistep synthesis from the brominated 1-bromo-3,5-xylene precursors and the corresponding 2-fluorenylaldehyde *via* Horner-Wadsworth-Emmons reactions followed by carbonylation using butyllithium and DMF.

1-bromo-3,5-bis(bromomethyl)benzene. Commercial 1-bromo-3,5-xylene (5.0 g, 3.67 mL, 27.02 mmol, 1 eq) was added into CH_2Cl_2 (100 mL, distilled), together with NBS (9.6 g, 54.04 mmol, 2 eq) and AIBN (220 mg, 1.35 mmol, 0.05 eq). The mixture was stirred for 30 min at room temperature, and then refluxed for 30 h. Then cooled in ice-water bath and filtered, washing residue with heptane. The solvents were evaporated and the residue was further purified by chromatography (heptane), collecting the target product (4.56 g, 49% yield) admixed with 1-bromo-3-bromomethyl-5-methylbenzene (20%) as white powder, as well as pure 1-bromo-3-bromomethyl-

5-methylbenzene (3.55 g) and 1-bromo-3-(bromomethyl)-5-(dibromomethyl)benzene (1.4 g). ^1H NMR (400 MHz, CDCl_3 , ppm): δ 7.47 (s, 2H), 7.34 (s, 1H), 4.41 (s, 4H).

Tetraethyl (5-bromo-1,3-phenylene)bis (methylene)diphosphonate (3). In a flask, the previously isolated [4:1] mixture of 1-bromo-3,5-bromomethyl-benzene and 1-bromo-3-bromomethyl-5-methylbenzene (2.4 g, 7 mmol, 1 eq) and $\text{P}(\text{OEt})_3$ (2.4 mL, 14 mmol, 2 eq) were added, respectively. The mixture was refluxed for 4 h at 140 °C. The excess of $\text{P}(\text{OEt})_3$ was removed under reduced pressure. Then the title product was purified by chromatography using CH_2Cl_2 to remove other byproducts and then collected by ethyl acetate, giving a colorless oil (2.66 g, 83% yield). ^1H NMR (400 MHz, CDCl_3 , ppm): δ 7.34 (s, 2H), 7.16 (s, 1H), 4.07–4.00 (m, 8H), 3.08 (d, $J = 22.0$ Hz, 4H), 1.26 (t, $J = 7.0$ Hz, 12 H).

Intermediate D1-PhBr. In a Schlenk tube, fluorenylaldehyde **1** (1.69 g, 5.51 mmol, 2.2 eq) and previously obtained **3** (1.15 g, 2.51 mmol, 1 eq) were added, then THF (100 mL, dried) was injected. After cooling the Schlenk with an ice-water bath (0 °C), *t*-BuOK (1.20 g, 10.69 mmol, 4.4 eq) was added under Argon and the reaction was kept stirring for 1 h at 0 °C. The bath was removed, a saturated NH_4Cl solution (aq) added and the resulting solution extracted with ethyl acetate. After evaporating the solvents, it was further purified by chromatography (CH_2Cl_2 /heptane [1:10]), giving **D1-PhBr** as a white powder (1.7 g, 89% yield). ^1H NMR (400 MHz, CDCl_3 , ppm): δ 7.71 (d, $J = 7.6$ Hz, 4H), 7.61 (s, 1H), 7.60 (s, 2H), 7.52 (d, $J = 8.4$ Hz, 2H), 7.50 (s, 2H), 7.37–7.31 (m, 6H), 7.27 (d, $J = 16.0$ Hz, 2H), 7.12 (d, $J = 16.4$ Hz, 2H), 2.01 (t, $J = 8.0$ Hz, 8H), 1.15–1.06 (m, 8 H), 0.71–0.58 (m, 20H).

Dendron D1-PhCHO. In a Schlenk tube, **D1-PhBr** (720 mg, 0.94 mmol, 1 eq) was dissolved in THF (60 mL) and *n*-BuLi (0.59 mL, 0.94 mmol, 1.6 M, 1 eq) was added dropwise at –78 °C during 15 min. The reaction was stirred for additional 40 min at low temperature. Then DMF (1 mL, dried) was added and stirring was continued for 1 h at –78 °C. The bath was removed, a saturated NH_4Cl solution (aq) added and the resulting solution extracted with ethyl acetate. After evaporating the solvents, it was further purified by chromatography (CH_2Cl_2 /heptane [1:5]), giving **D1-PhCHO** as a light-yellow powder (580 mg, 86% yield).

^1H NMR (400 MHz, CDCl_3 , ppm): δ 10.11 (s, 1H), 7.96 (s, 3H), 7.73–7.71 (m, 4H), 7.56 (d, $J = 8.0$ Hz, 2H), 7.53 (s, 2H), 7.40–7.23 (m, 10H), 2.02 (t, $J = 8.0$ Hz, 8H), 1.15–1.06 (m, 8 H), 0.71–0.56 (m, 20H). HRMS-ESI: m/z calcd for $\text{C}_{53}\text{H}_{58}\text{O}$: 710.44822 $[\text{M}]^+$; found 710.4481.

Intermediate D2-PhBr. This synthesis is a classical procedure similar to that previously used for **D1-PhBr**. The purification was completed by chromatography (heptane/ CH_2Cl_2 [10:1]), providing **D2-PhBr** as a white powder (93% yield). ^1H NMR (400 MHz, CDCl_3 , ppm): δ 7.72–7.71 (m, 10H), 7.64 (s, 7H), 7.57 (d, $J = 8.0$ Hz, 4H), 7.55 (s, 4H), 7.37–7.31 (m, 16H), 7.30–7.18 (m, 8H), 2.03 (t, $J = 8.0$ Hz, 16H), 1.16–1.07 (m, 16 H), 0.72–0.57 (m, 40H).

Dendron D2-PhCHO. This synthesis is a classical procedure similar to that previously used for **D1-PhCHO**. The purification was completed by chromatography (heptane/ CH_2Cl_2 [5:1]), providing **D2-PhCHO** as a yellow powder (65% yield). ^1H NMR (400 MHz, CD_2Cl_2 , ppm): δ 10.15 (s, 1H), 8.05 (s, 3H), 7.76–7.73 (m, 13H), 7.62–7.59 (m, 8H), 7.42–7.29 (m, 25H), 2.06 (t, $J = 8.0$ Hz, 16H), 1.17–1.08 (m, 16 H), 0.72–0.54 (m, 40H). HRMS-ESI: m/z calcd for $\text{C}_{115}\text{H}_{122}\text{O}$: 1518.94902 $[\text{M}]^+$; found 1518.9487.

3.3. Porphyrin synthesis and characterization

Reference porphyrins **TPP**, **TPP-T1**, and **TPP-T2** were synthesized as described earlier by our group [32,40]. The generation G1 dendrimer **TPP-D1** was obtained under Adler–Longo conditions as described earlier (8% yield) [28].

ZnTPP-D1. The free-base porphyrin **TPP-D1** reacts with excess of $\text{Zn}(\text{OAc})_2$ in [3:1] mixture of CH_2Cl_2 and MeOH at 40 °C overnight. After evaporating the solvents, **ZnTPP-D1** was purified by chromatography (petroleum ether/ CH_2Cl_2 [5:1]) and after evaporation of the volatiles was obtained as a pink powder (80% yield). ^1H NMR (400 MHz, CD_2Cl_2 , ppm): δ 9.20 (s, 8H), 8.42 (s, 8H), 8.21 (s, 4H), 7.71–7.68 (m, 32H), 7.60–7.54 (m, 60H), 7.48 (d, $J = 8.4$ Hz, 8H), 7.42–7.27 (m, 80H), 7.15 (dd, $J_1 = 8.4$ Hz, $J_2 = 2.4$ Hz, 4H), 2.01 (t, $J = 7.2$ Hz, 64H), 1.12–1.01 (m, 64H), 0.65–0.51 (m, 160H) [28]. ^{13}C NMR (125 MHz, CDCl_3 , ppm): δ 151.3, 151.0, 143.0, 141.2, 140.8, 136.3, 136.1, 132.0, 130.7, 127.6, 127.1, 126.8, 125.8, 124.0, 122.8, 120.8, 119.9, 119.7, 54.9, 40.3, 25.9, 23.1,

13.8. HRMS MALDI: m/z calcd for $\text{C}_{228}\text{H}_{236}\text{N}_4\text{Zn}$: 3093.7876 $[\text{M}]^+$; found 3093.782.

Dendrimer TPP-D2. The mixture of **D2-PhCHO** (250 mg, 0.16 mmol, 1 eq) and propionic acid (4 mL) was heated to 120 °C. After pyrrole (0.01 mL, 0.16 mmol, 1 eq) in propionic acid (1 mL) was added into the mixture dropwise, the reaction was kept refluxing for 5.5 h. After cooling to room temperature, MeOH was then added to the reaction mixture and the precipitate was filtered. The residue could be purified by chromatography (petroleum ether/ CH_2Cl_2 [5:1]) as a red powder (10 mg, 4% yield). ^1H NMR (400 MHz, CD_2Cl_2 , ppm): δ 9.10 (broad s, 8H), 8.50 (s, 8H), 8.20–7.10 (large signals, 188H), 2.01 (large s, 64H), 1.00 (m, 64H), 0.60–0.50 (m, 160H).

ZnTPP-D2. Previous crude mixture **TPP-D2** (10 mg, 1.6×10^{-6} mol, 1 eq) reacts with excess of $\text{Zn}(\text{OAc})_2$ (3 mg, 1.6×10^{-5} mol, 10 eq) in a [3:1] mixture of CH_2Cl_2 and MeOH (1 mL) at 40 °C overnight. After evaporating the solvents, the Zn complex **ZnTPP-D2** could be isolated by chromatography (petroleum ether/ CH_2Cl_2 [5:1]), as a pink powder (60% yield). ^1H NMR (400 MHz, CD_2Cl_2 , ppm): δ 9.20 (s, 8H), 8.42 (s, 8H), 8.21 (s, 4H), 7.71–7.68 (m, 32H), 7.60–7.54 (m, 60H), 7.48 (d, $J = 8.4$ Hz, 8H), 7.42–7.27 (m, 80H), 7.15 (dd, $J_1 = 8.4$ Hz, $J_2 = 2.4$ Hz, 4H), 2.01 (t, $J = 7.2$ Hz, 64H), 1.12–1.01 (m, 64H), 0.65–0.51 (m, 160H).

3.4. Spectroscopic measurements

All measurements have been performed with freshly prepared air-equilibrated solutions at room temperature (298 K). Fluorescence measurements were performed on dilute solutions (*ca.* 10^{-6} M, optical density < 0.1) contained in standard 1 cm quartz cuvettes. Fully corrected emission spectra were obtained, for each compound, under excitation at the wavelength of the absorption maximum, with $A_{\lambda\text{ex}} < 0.1$ to minimize internal absorption.

Measurements of singlet oxygen quantum yield (Φ_Δ). Measurements were performed on a Fluorolog-3 (Horiba Jobin Yvon), using a 450 W Xenon lamp. The emission at 1272 nm was detected using a liquid nitrogen-cooled Ge-detector model (EO-817L, North Coast Scientific Co). Singlet oxygen quantum yields Φ_Δ were determined in dichloromethane solutions, using tetraphenylporphyrin (**TPP**) in dichloromethane as reference solution (Φ_Δ [TPP]

= 0.60) and were estimated from $^1\text{O}_2$ luminescence at 1272 nm.

Two-Photon Absorption Experiments. To span the 790–920 nm range, a Nd:YLF-pumped Ti:sapphire oscillator (Chameleon Ultra, Coherent) was used generating 140 fs pulses at a 80 MHz rate. The excitation power is controlled using neutral density filters of varying optical density mounted in a computer-controlled filter wheel. After five-fold expansion through two achromatic doublets, the laser beam is focused by a microscope objective (10 \times , NA 0.25, Olympus, Japan) into a standard 1 cm absorption cuvette containing the sample. The applied average laser power arriving at the sample is typically between 0.5 and 40 mW, leading to a time-averaged light flux in the focal volume on the order of 0.1–10 mW/mm 2 . The fluorescence from the sample is collected in epifluorescence mode, through the microscope objective, and reflected by a dichroic mirror (Chroma Technology Corporation, USA; “blue” filter set: 675dcxru; “red” filter set: 780dxcr). This makes it possible to avoid the inner filter effects related to the high dye concentrations used (10^{-4} M) by focusing the laser near the cuvette window. Residual excitation light is removed using a barrier filter (Chroma Technology; “blue”: e650–2p, “red”: e750sp–2p). The fluorescence is coupled into a 600 μm multimode fiber by an achromatic doublet. The fiber is connected to a compact CCD-based spectrometer (BTC112-E, B&W Tek, USA), which measures the two-photon excited emission spectrum. The emission spectra are corrected for the wavelength dependence of the detection efficiency using correction factors established through the measurement of reference compounds having known fluorescence emission spectra. Briefly, the setup allows for the recording of corrected fluorescence emission spectra under multiphoton excitation at variable excitation power and wavelength. TPA cross-sections (σ_2) were determined from the two-photon excited fluorescence (TPEF) cross-sections ($\sigma_2 \cdot \Phi_F$) and the fluorescence emission quantum yield (Φ_F). TPEF cross-sections of 10^{-4} M CH_2Cl_2 solutions were measured relative to fluorescein in 0.01 M aqueous NaOH using the well-established method described by Xu and Webb [39,43] and the appropriate solvent-related refractive index corrections [55]. The quadratic dependence of the fluorescence intensity on the exci-

tation power was checked for each sample and all wavelengths.

4. Conclusions

We report here the synthesis, characterization, and a photochemical study of two new zinc(II) complexes of **TPP**-based dendritic chromophores possessing 8 to 12 fluorenyl groups at their periphery (**ZnTPP-D1** and **ZnTPP-D2**). The corresponding free-base porphyrins are analogs of related dendrimers in which we have now replaced the alkyne linkages (**T** series) by *E*-alkene ones (**D** series) at their periphery (Scheme 1). While **TPP-D2** could not be isolated pure, metalation of this free base by Zn(II) provided a convenient mean to selectively access a representative of the higher generation dendrimer (**ZnTPP-D2**). Comparison with previously gathered data indicate that the optical properties of these dendrimers exhibit an obvious dependence on the dendrimer structure, *E*-alkene linkers being clearly better than 1,2-alkyne ones for enhancing the photo-physical properties of interest (luminescence, 2PA cross-section, and sensitization yields) for performing 2P-PDT and fluorescence imaging. Comparison between **TPP-D1** and **ZnTPP-D1** also reveals that metalation does not drastically affect the two-photon absorption cross-section nor improve the oxygen-sensitizing efficiency of these dendrimers.

Acknowledgments

The authors acknowledge China Scholarship Council (CSC) for PhD funding (DY, LS, and XZ). This project was supported by the departmental committees CD35, CD28, and CD29 of the “*Ligue contre le Cancer du Grand-Ouest*.”

Supplementary data

Supporting information for this article is available on the journal’s website under <https://doi.org/10.5802/crchim.99> or from the author.

References

- [1] R. J. Abraham, G. E. Hawkes, M. F. Hudson, K. M. Smith, *J. Chem. Soc., Perkin. Trans. II*, 1975, 204–211.
- [2] H. N. Fonda, J. V. Gilbert, R. A. Cormier, J. R. Sprague, K. Kamioka, J. S. Connolly, *J. Phys. Chem.*, 1993, **97**, 7024–7033.

- [3] A. Toeibs, N. Haeberle, *Justus Liebigs Ann. Chem.*, 1968, **718**, 183-187.
- [4] E. M. Harth, S. Hecht, B. Helms, E. E. Malmstrom, J. M. Fréchet, C. J. Hawker, *J. Am. Chem. Soc.*, 2002, **124**, 3926-3938.
- [5] W. R. Dichtel, J. M. Serin, C. Edde, J. M. Fréchet, *J. Am. Chem. Soc.*, 2004, **126**, 5380-5381.
- [6] M. A. Oar, J. M. Serin, J. M. Fréchet, *Chem. Mater.*, 2006, **18**, 3682-3692.
- [7] B. Li, J. Li, Y. Fu, Z. Bo, *J. Am. Chem. Soc.*, 2004, **126**, 3430-3431.
- [8] B. Li, X. Xu, M. Sun, Y. Fu, G. Yu, Y. Liu, Z. Bo, *Macromolecules*, 2006, **39**, 456-461.
- [9] M. Sun, Z. Bo, *J. Polym. Sci.: Part A: Polym. Chem.*, 2006, **45**, 111-124.
- [10] C. O. Paul-Roth, G. Simonneaux, *Tetrahedron Lett.*, 2006, **47**, 3275-3278.
- [11] C. O. Paul-Roth, G. Simonneaux, *C. R. Acad. Sci. Ser. IIb: Chim.*, 2006, **9**, 1277-1286.
- [12] C. Paul-Roth, G. Williams, J. Letessier, G. Simonneaux, *Tetrahedron Lett.*, 2007, **48**, 4317-4322.
- [13] S. Drouet, C. Paul-Roth, G. Simonneaux, *Tetrahedron*, 2009, **65**, 2975-2981.
- [14] S. Drouet, C. O. Paul-Roth, *Tetrahedron*, 2009, **65**, 10693-10700.
- [15] A. Merhi, S. Drouet, N. Kerisit, C. O. Paul-Roth, *Tetrahedron*, 2012, **68**, 7901-7910.
- [16] D. Yao, V. Hugues, M. Blanchard-Desce, O. Mongin, C. O. Paul-Roth, F. Paul, *New J. Chem.*, 2015, **39**, 7730-7733.
- [17] D. Yao, X. Zhang, O. Mongin, F. Paul, C. O. Paul-Roth, *Chem. Eur. J.*, 2016, **22**, 5583-5597.
- [18] L. B. Josefsen, R. W. Boyle, *Theranostics*, 2012, **2**, 916-966.
- [19] P.-C. Lo, M. S. Rodriguez-Morgade, R. K. Pandey, D. K. P. Ng, T. Torres, F. Dumoulin, *Chem. Soc. Rev.*, 2020, **49**, 1041-1056.
- [20] Z. Sun, L.-P. Zhang, F. Wu, Y. Zhao, *Adv. Funct. Mater.*, 2017, **27**, article no. 1704079.
- [21] F. Bolze, S. Jenni, A. Sour, V. Heitz, *Chem. Commun.*, 2017, **53**, 12857-12877.
- [22] M. Khurana, H. A. Collins, A. Karotki, H. L. Anderson, D. T. Cramb, B. C. Wilson, *Photochem. Photobiol.*, 2007, **83**, 1441-1448.
- [23] J. Schmitt, S. Jenni, A. Sour, V. Heitz, F. Bolze, A. Pallier, C. S. Bonnet, É. Tóth, B. Ventura, *Bioconjug. Chem.*, 2018, **29**, 3726-3738.
- [24] J. R. Starkey, E. M. Pascucci, M. A. Drobizhev, A. Elliott, A. K. Rebane, *Biochim. Biophys. Acta*, 2013, **1830**, 4594-4603.
- [25] H. A. Collins, M. Khurana, E. H. Moriyama, A. Mariampillai, E. Dahlstedt, M. Balaz, M. K. Kuimova, M. Drobizhev, V. X. D. Yang, D. Phillips, A. Rebane, B. C. Wilson, H. L. Anderson, *Nat. Photonics*, 2008, **2**, 420-424.
- [26] L. Shi, C. Nguyen, M. Daurat, A. C. Dhieb, W. Smirani, M. Blanchard-Desce, M. Gary-Bobo, O. Mongin, C. Paul-Roth, F. Paul, *Chem. Commun.*, 2019, **55**, 12231-12234.
- [27] F. Paul, C. Lapinte, *Coord. Chem. Rev.*, 1998, **178/180**, 431-480.
- [28] D. Yao, X. Zhang, S. Abid, L. Shi, M. Blanchard-Desce, O. Mongin, F. Paul, C. O. Paul-Roth, *New J. Chem.*, 2018, **42**, 395-401.
- [29] L. Rigamonti, B. Babgi, M. P. Cifuentes, R. L. Roberts, S. Petrie, R. Stranger, S. Righetto, A. Teshome, I. Asselberghs, K. Clays, M. G. Humphrey, *Inorg. Chem.*, 2009, **48**, 3562-3572.
- [30] S. Yao, H.-Y. Ahn, X. Wang, J. Fu, E. W. Van Stryland, D. J. Hagan, K. D. Belfield, *J. Org. Chem.*, 2010, **75**, 3965-3974.
- [31] G. Mehta, P. Sarma, *Tetrahedron Lett.*, 2002, **43**, 9343-9346.
- [32] O. Hassan Omar, F. Babudri, G. M. Farinola, F. Naso, A. Operamolla, *Eur. J. Org. Chem.*, 2011, 529-537.
- [33] A. D. Adler, F. R. Longo, J. D. Finarelli, J. Assour, L. Korsakoff, *J. Org. Chem.*, 1967, **32**, 476-476.
- [34] A. D. Adler, F. R. Longo, W. Shergalis, *J. Am. Chem. Soc.*, 1964, **86**, 3145-3149.
- [35] J. S. Lindsey, I. C. Schreiman, H. C. Hsu, P. C. Kearney, A. M. Marguerettaz, *J. Org. Chem.*, 1987, **52**, 827-836.
- [36] D. Yao, X. Zhang, A. Triadon, N. Richey, O. Mongin, M. Blanchard-Desce, F. Paul, C. O. Paul-Roth, *Chem. Eur. J.*, 2017, **23**, 2635-2647.
- [37] M. Gouterman, *J. Mol. Spectrosc.*, 1961, **6**, 138-163.
- [38] E. Austin, M. Gouterman, *Bioinorg. Chem.*, 1978, **9**, 281-298.
- [39] N. S. Makarov, M. Drobizhev, A. Rebane, *Opt. Exp.*, 2008, **16**, 4029-4047.
- [40] M. Gouterman, *The Porphyrins*, vol. 3, Academic Press, New-York, 1978.
- [41] J. Griffiths, *Colour and Constitution of Organic Molecules*, Academic Press Inc., London, 1976.
- [42] D. Cao, L. Zhu, Z. Liu, W. Lin, *J. Photochem. Photobiol. C: Photochem. Rev.*, 2020, **44**, article no. 100371.
- [43] C. Xu, W. W. Webb, *J. Opt. Soc. Am. B*, 1996, **13**, 481-491.
- [44] M. Drobizhev, Y. Stepanenko, Y. Dzenis, A. Karotki, A. Rebane, P. N. Taylor, H. L. Anderson, *J. Am. Chem. Soc.*, 2004, **126**, 15352-15353.
- [45] D. Y. Kim, T. K. Ahn, J. H. Kwon, D. Kim, T. Ikeue, N. Aratani, A. Osuka, M. Shigeiwa, S. Maeda, *J. Phys. Chem. A*, 2005, **109**, 2996-2999.
- [46] M. Drobizhev, Y. Stepanenko, Y. Dzenis, A. Karotki, A. Rebane, P. N. Taylor, H. L. Anderson, *J. Phys. Chem. B*, 2005, **109**, 7223-7236.
- [47] T. K. Ahn, K. S. Kim, D. Y. Kim, S. B. Noh, N. Aratani, C. Ikeda, A. Osuka, D. Kim, *J. Am. Chem. Soc.*, 2006, **128**, 1700-1704.
- [48] K. Ogawa, H. Hasegawa, Y. Inaba, Y. Kobuke, H. Inouye, Y. Kanemitsu, E. Kohno, T. Hirano, S.-I. Ogura, I. Okura, *J. Med. Chem.*, 2006, **49**, 2276-2283.
- [49] S. Achelle, P. Couleaud, P. Baldeck, M.-P. Teulade-Fichou, P. Maillard, *Eur. J. Org. Chem.*, 2011, **2011**, 1271-1279.
- [50] F. Hammerer, S. Achelle, P. Baldeck, P. Maillard, M.-P. Teulade-Fichou, *J. Phys. Chem. A*, 2011, **115**, 6503-6508.
- [51] M. Pawlicki, M. Morisue, N. K. S. Davis, D. G. McLean, J. E. Haley, E. Beuerman, M. Drobizhev, A. Rebane, A. L. Thompson, S. I. Pascu, G. Accorsi, N. Armaroli, H. L. Anderson, *Chem. Sci.*, 2012, **3**, 1541-1547.
- [52] S. J. Silvers, A. Tulinsky, *J. Am. Chem. Soc.*, 1967, **89**, 3331-3337.
- [53] O. Mongin, V. Hugues, M. Blanchard-Desce, A. Merhi, S. Drouet, D. Yao, C. Paul-Roth, *Chem. Phys. Lett.*, 2015, **625**, 151-156.
- [54] D. D. Perrin, W. L. F. Armarego, *Purification of Laboratory Chemicals*, 3rd ed., Pergamon Press, Oxford, 1988.
- [55] M. H. V. Werts, N. Nerambourg, D. Pélégry, Y. Le Grand, M. Blanchard-Desce, *Photochem. Photobiol. Sci.*, 2005, **4**, 531-538.